

ARTICLE

Structural and Magnetic Properties of $\text{Bi}(\text{Fe}_{1-x}\text{Mn}_x)\text{O}_3$

Bin-feng Ding*

Department of Physics and Electronic Information, Langfang Teachers College, Langfang 065000, China

(Dated: Received on November 27, 2011; Accepted on February 12, 2012)

$\text{Bi}(\text{Fe}_{1-x}\text{Mn}_x)\text{O}_3$ bulk ceramics with Mn concentration x up to 0.3 were prepared by rapid sintering using sol-gel derived fine powders. Structure transformation is found to depend on the Mn doping concentration by X-ray diffraction and Raman spectroscopy. $\text{Bi}(\text{Fe}_{1-x}\text{Mn}_x)\text{O}_3$ maintains the rhombohedral structure of BiFeO_3 with $x=0.05$ and 0.1, but changes to the orthorhombic structure with $x=0.3$. Weak ferromagnetism is observed for $\text{Bi}(\text{Fe}_{1-x}\text{Mn}_x)\text{O}_3$ with $x=0.05$ and 0.1, but stronger paramagnetism is observed for $\text{Bi}(\text{Fe}_{1-x}\text{Mn}_x)\text{O}_3$ with $x=0.3$ indicating a magnetic phase change from antiferromagnetic to paramagnetic with the structure changing from R3c to C222. Two anomalies at 30 and 140 K are observed for $\text{Bi}(\text{Fe}_{1-x}\text{Mn}_x)\text{O}_3$ with $x=0.05$ and 0.1. The anomaly at 30 K is concluded to be related to the freezing of cluster spin glass from dc magnetic memory and relaxation measurements.

Key words: Multiferroic, Spin glass, Ferromagnetism, Cluster**I. INTRODUCTION**

Multiferroic materials have simultaneously at least two ferroic orderings, such as ferromagnetism, ferroelectricity, ferroelasticity, and ferrotoroidicity, which enable a coupling interaction between them and provides novel functions [1]. However, due to the mutual exclusion of the ferromagnetism and ferroelectricity, there are very new single phase multiferroic materials [2]. Among them, R3c BiFeO_3 (BFO) is one of the most widely studied multiferroic materials for its above room temperature (RT) magnetic Néel temperature ($T_N \approx 643$ K) and ferroelectric Curie temperature ($T_C \approx 1103$ K) [3]. Enhanced ferroelectric polarization with remnant polarization P_r of $\sim 60 \mu\text{C}/\text{cm}^2$ has been reported in high quality epitaxial BFO films and single crystals [4, 5]. However, the large leakage current of BFO thin films at RT is known to be a serious problem, which could limit the various applications of this material [6]. On the other hand, BFO has a superimposed incommensurate cycloid spin structure with a periodicity of about 64 nm [7]. This structure decreases the macroscopic magnetization and inhibits the observation of the linear magnetoelectric effect [8].

As a solution, ion substitution is a general method to suppress the leakage current and induce RT ferromagnetism in BFO [9–11]. A ferroelectric to paraelectric phase transition besides the release of weak ferromagnetism has been observed in La-doped BFO with structure changing from R3c to pseudotetragonal symmetry

[12]. Mn has been clearly demonstrated to be effective in suppressing the leakage current and in improving the ferroelectricity in BiFeO_3 , but a systematic magnetic investigation is still rare [13]. Furthermore, the low temperature anomalies in the magnetic properties of BFO are still open questions [14].

In this work, we study detailed structural and magnetic on $\text{Bi}(\text{Fe}_{1-x}\text{Mn}_x)\text{O}_3$ with $x=0.05$, 0.1 and 0.3. The low temperature magnetic anomaly at 30 K has been demonstrated to be related to the freezing of cluster spin glass.

II. EXPERIMENTS

$\text{Bi}(\text{Fe}_{1-x}\text{Mn}_x)\text{O}_3$ ($x=0.05$, 0.1 and 0.3) ceramics were prepared by sol-gel method with rapid sintering process. Appropriate amounts of $\text{Bi}(\text{NO}_3)_3 \cdot 5\text{H}_2\text{O}$, $\text{Fe}(\text{NO}_3)_3 \cdot 9\text{H}_2\text{O}$, and $\text{Mn}(\text{NO}_3)_2$ were dissolved in ethylene glycol. The obtained solutions were dried at 80 °C, and then sintered at 450 °C in air for 24 h. The obtained powders were grinded, and pressed into 1 mm thick disks with a diameter of 13 mm. The disks were directly put into an 800 °C oven and sintered in air for 20 min. The sintered disks were taken out from the oven and cooled to room temperature within several minutes. The structure of samples was studied by X-ray diffraction (XRD) with $\text{Cu K}\alpha$ radiation and scanning electron microscopy (SEM) measurements. Raman measurements were carried out on a Horiba Jobin Yvon LabRAM HR 800 micro-Raman spectrometer with 785 nm excitation source under air ambient conditions at room temperature. The laser was focused on the sample surface with a diameter of 1 μm . The magnetic properties were measured by a physical property

* Author to whom correspondence should be addressed. E-mail: ding_binfeng@126.com

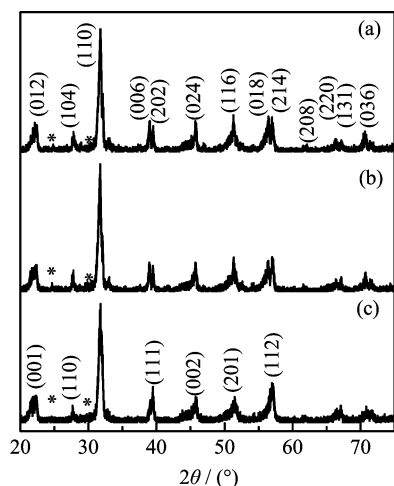


FIG. 1 XRD patterns of $\text{Bi}(\text{Fe}_{1-x}\text{Mn}_x)\text{O}_3$ bulk ceramics with (a) $x=0.05$, (b) $x=0.1$, and (c) $x=0.3$. The stars mark the impurity phase of $\text{Bi}_{25}\text{FeO}_{39}$.

measurement system (PPMS-9, Quantum Design) and a superconducting quantum interference device magnetometer (SQUID) with fields up to 7 T and in the temperature range from 4 K to 350 K.

III. RESULTS AND DISCUSSION

The XRD patterns of the sintered $\text{Bi}(\text{Fe}_{1-x}\text{Mn}_x)\text{O}_3$ ceramics are shown in Fig.1. It can be seen that $\text{Bi}(\text{Fe}_{1-x}\text{Mn}_x)\text{O}_3$ with $x=0.05$ and 0.1 mainly exhibits the rhombohedral structure (R3c). However, small impurity peaks marked by stars at 2θ around 30° have been observed in all the samples, which are identified to be from $\text{Bi}_{25}\text{FeO}_{39}$. This impurity phase is always the byproduct obtained during the preparation of BiFeO_3 ceramics [15]. It should be noted that the diffraction intensity from the impurity phase keeps almost unchanged and comparable to that in BiFeO_3 [16], indicating that the formation of $\text{Bi}_{25}\text{FeO}_{39}$ is not from the Mn substitution. A significant structure change has been observed in the sample with $x=0.3$. The split diffraction peaks around $2\theta=32^\circ$, 39° , and 57° in the XRD patterns of $\text{Bi}(\text{Fe}_{1-x}\text{Mn}_x)\text{O}_3$ with $x=0.05$, 0.1 merge into a single diffraction peak when $x=0.3$: *i.e.* the structure changes from rhombohedral (R3c) to orthorhombic structure. Similar phenomenon has been observed in the La doped BFO with La doping concentration of 0.2 , and the structure has C222 orthorhombic symmetry [17].

Figure 2 shows the SEM images of $\text{Bi}(\text{Fe}_{1-x}\text{Mn}_x)\text{O}_3$ ceramics. The grain size of $\text{Bi}(\text{Fe}_{0.95}\text{Mn}_{0.05})\text{O}_3$ is fairly uniform and estimated to be about $1\ \mu\text{m}$. With increasing the Mn concentration to 0.1 , the grain size distribution becomes rather nonuniform. And the size of grains is estimated to be about $500\ \text{nm}$. With further increasing Mn concentration to 0.3 , the grain size and distri-

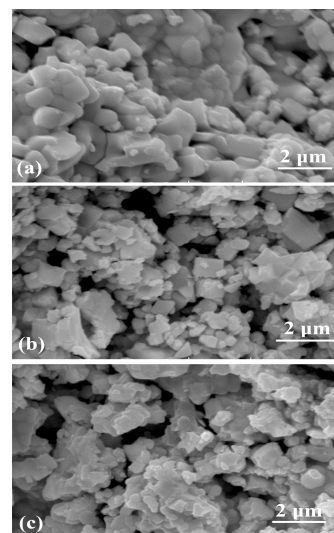


FIG. 2 SEM images of $\text{Bi}(\text{Fe}_{1-x}\text{Mn}_x)\text{O}_3$ bulk ceramics with (a) $x=0.05$, (b) $x=0.1$, and (c) $x=0.3$.

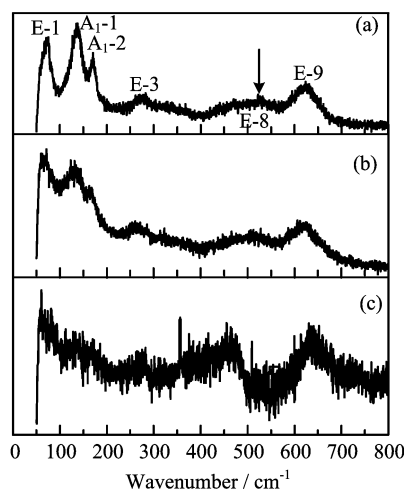


FIG. 3 Raman spectra of $\text{Bi}(\text{Fe}_{1-x}\text{Mn}_x)\text{O}_3$ bulk ceramics with (a) $x=0.05$, (b) $x=0.1$, and (c) $x=0.3$.

bution change little compared with $\text{Bi}(\text{Fe}_{0.9}\text{Mn}_{0.1})\text{O}_3$.

Details of the structural evolution of BiFeO_3 with ion substitution can be probed more explicitly through Raman spectra [18]. The Raman spectra of samples are shown in Fig.3. The clearly resolved Raman modes of R3c $\text{Bi}(\text{Fe}_{0.95}\text{Mn}_{0.05})\text{O}_3$ are marked by arrows in Fig.3, which can all be indexed to the modes of BiFeO_3 molecules [19–21]. As the intensity of the Raman peaks of BiFeO_3 decreases with increasing temperature, not all modes can be clearly observed above RT [22]. With increasing Mn concentration to 0.1 , the intensity of each mode becomes weak, though both samples exhibit similar structure from XRD patterns. This indicates the deterioration of the crystalline structure of BiFeO_3 with increasing Mn substitution. With 0.3 Mn substitution, the structure has changed from R3c to C222, thus most

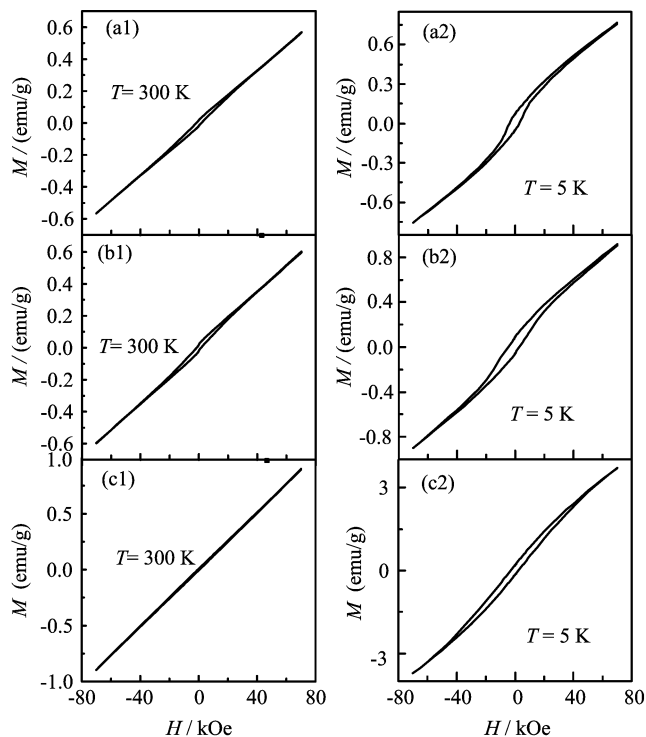


FIG. 4 Magnetic hysteresis loops measured at 300 and 5 K of $\text{Bi}(\text{Fe}_{1-x}\text{Mn}_x)\text{O}_3$ bulk ceramics with (a) $x=0.05$, (b) $x=0.1$, and (c) $x=0.3$.

modes of BiFeO_3 disappear. As predicted theoretically, due to the magnetoelectric and spin-phonon interaction Raman spectra probed on BiFeO_3 may also reveal strong anomalies around the magnetic and electric phase transition temperatures T_N and T_C , respectively [23]. As expected we see no anomaly in the RT Raman spectra because none of the samples has its magnetic or electric phase transition temperature at RT.

Figure 4 shows the room temperature magnetic hysteresis loops for $\text{Bi}(\text{Fe}_{1-x}\text{Mn}_x)\text{O}_3$ ceramics. Weak ferromagnetism is observed for $\text{Bi}(\text{Fe}_{0.95}\text{Mn}_{0.05})\text{O}_3$. With the Mn concentration increasing to 0.1, similar weak ferromagnetism is observed. However, with further increasing Mn concentration to 0.3, the sample exhibits nearly linear M - H curve, indicating the paramagnetism in $\text{Bi}(\text{Fe}_{0.7}\text{Mn}_{0.3})\text{O}_3$. An interesting phenomenon is the increasing magnetization with increasing Mn concentration, which is most significant at 5 K from the M - H curves shown in the right panel of Fig.4. All the samples exhibit weak ferromagnetism at 5 K.

Figure 5 shows the temperature dependent magnetization curves for $\text{Bi}(\text{Fe}_{1-x}\text{Mn}_x)\text{O}_3$ ceramics. Zero field cooled (ZFC) and field cooled (FC) temperature dependent magnetization curves were measured under 1 kOe from 5 K to 300 K with cooling field of 1 kOe for FC measurements. For $\text{Bi}(\text{Fe}_{0.7}\text{Mn}_{0.3})\text{O}_3$, the magnetization for both the FC and ZFC curve increases with decreasing temperature, indicating the paramagnetism (Fig.5(c)). The slight difference between ZFC

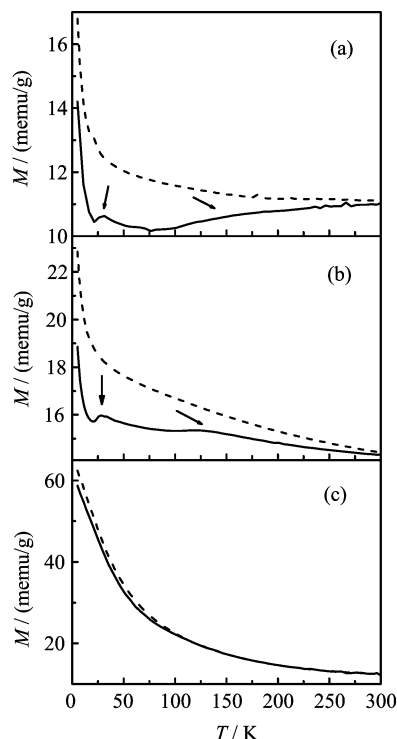


FIG. 5 FC (dashed lines) and ZFC (solid lines) magnetization of $\text{Bi}(\text{Fe}_{1-x}\text{Mn}_x)\text{O}_3$ bulk ceramics with (a) $x=0.05$, (b) $x=0.1$, and (c) $x=0.3$. The arrows exhibit the difference of 2 peaks (one at around 30 K and the other around 140 K) between ZFC and FC curves for $\text{Bi}(\text{Fe}_{1-x}\text{Mn}_x)\text{O}_3$ with $x=0.05$ and 0.1.

and FC curves below about 100 K indicates the weak ferromagnetism at low temperature, as shown in the M - H curve at 5 K. For $\text{Bi}(\text{Fe}_{1-x}\text{Mn}_x)\text{O}_3$ with $x=0.05$ and 0.1 the FC magnetization continues to increase with decreasing temperature. Interestingly, the ZFC curve bifurcates from the FC one below 350 K and exhibits two peaks (one at around 30 K and the other around 140 K). The two peaks can be observed more clearly for $\text{Bi}(\text{Fe}_{0.9}\text{Mn}_{0.1})\text{O}_3$, thus we concentrate on this sample in the following studies.

We performed history-dependent magnetic memory measurements using a cooling and waiting protocol suggested by Sun *et al.* [24]. The sample was cooled at 1 kOe and the magnetization was measured with cooling, but temporarily stopped at 150, 100, 50, and 20 K for a waiting period of 2 h. During waiting, the field was set to zero. After the stop, the 1 kOe field was re-applied and cooling and measuring were resumed. The temporary stops resulted in a step like M - T curve (solid line) in Fig.6. After reaching 4 K, the sample was heated back in the same field, and the magnetization was recorded again (circle). During the heating the M - T curve also has a step like behavior at 20 K. Thus, the system remembers its thermal history. The step like feature in the temperature dependent magnetization is a result of magnetic relaxation at the stopping

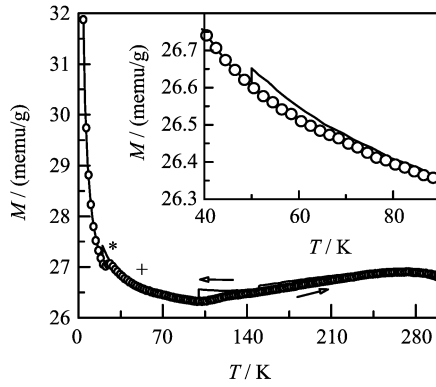


FIG. 6 Temperature dependent memory effect in the dc magnetization. The solid line is measured during the cooling in 1 kOe with a waiting period of 2 h at 150, 100, 50, and 20 K. The field is cut-off during stop. The open circles are measured with continuous heating at the same rate after the previous cooling protocol. Clear memory effect is observed at around 20 K, marked by “*”. The inset shows the enlarged view of the part marked by “+”.

point [24], and indicates the spin glass phase. There are no significant memory effects observed at other stopping temperatures, as can be seen clearly in the enlarged view of the stopping temperature of 50 K (inset of Fig.6). This precludes the spin glass transition at around 140 K.

To clearly understand the spin glass behavior in $\text{Bi}(\text{Fe}_{0.9}\text{Co}_{0.1})\text{O}_3$, the thermo-remnant magnetization (TRM) depending on time was measured at various temperatures below 350 K by cooling the sample in a field of 10 kOe from 350 K to the final temperature, abruptly decreasing the field to zero and observing the decay of remnant magnetization. For the cluster spin glass, a stretched exponential decay is expected [25–27],

$$M(t) = M_0 + M_r \exp \left[- \left(\frac{t}{\tau} \right)^{1-n} \right] \quad (1)$$

where the intrinsic ferromagnetic component M_0 and the glassy component M_r mainly contribute to the relaxation effects observed. The time t (normal time) and time constant τ (relaxation time) and exponent n (relaxation rate) are related to the relaxation rate of the cluster spin glass phase. The cluster spin glass behavior and its freezing temperature T_f can be determined from the TRM measurements, coinciding with the temperature dependent ac susceptibility measurement very well [25].

Figure 7(a) shows a typical relaxation curve measured at 5 K. The solid line is the fitting with Eq.(1). It can be clearly seen that the fitting to the experimental data is very good. On the other hand, for canonical spin glass, a linear relation was observed between M and $\ln t$ in the magnetic relaxation process [28]. As can be seen in the inset of Fig.7(a), the nonlinear relation between M and $\ln t$ excludes the possibility of canonical spin glass.

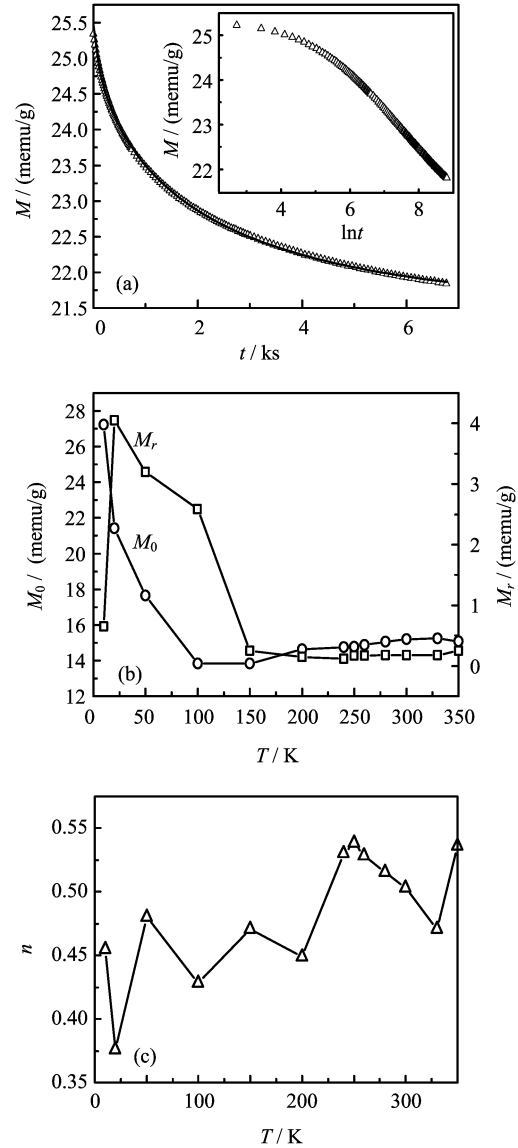


FIG. 7 (a) Measured (open symbol) and fitted (solid line) time dependent remnant magnetization at 20 K, the inset shows the magnetization in dependence on $\ln t$. (b) The temperature dependent M_0 , M_r . (c) The temperature dependent n .

By fitting the TRM curves at different temperatures, we can get the parameters M_0 , M_r , and n , as shown in Fig.7(b). n is close to 0.5 in the temperature range between 5 and 300 K, which is also an indication of the cluster spin glass [25–28]. M_0 and M_r depend strongly on temperature. The ferromagnetic component M_0 decreases with increasing temperature up to 150 K, and then increases with increasing temperature up to 350 K. The variation of the relaxation component M_r with T shows a peak at around 20 K, which roughly agrees with the anomalous temperature of 30 K from ZFC curve. The maximum in M_r coincides with the cluster freezing temperature [25]. Thus we can conclude the cluster

spin glass in $\text{Bi}(\text{Fe}_{0.9}\text{Mn}_{0.1})\text{O}_3$ with freezing temperature of about 30 K. There is no peak of M_r observed at around 140 K, indicating this magnetic anomaly is not related to the cluster spin glass. This might be explained by the spin reorientation, a similar anomaly has been observed in BiFeO_3 at around 150 K [29].

In previous study on $\text{Bi}(\text{Fe}_{0.95}\text{Co}_{0.05})\text{O}_3$, two freezing temperatures of cluster spin glass, one at 260 K and the other at 100 K, have been observed [21]. The higher T_f is related to the canted antiferromagnetic arranged spins between Fe ions, and the lower T_f is related to the ferrimagnetic arranged spins between Co and Fe ions. From Raman measurements, we have clarified that the structural distortion on Fe atomic sites by Co substitution is stronger than the structural distortion on Fe atomic sites by Mn substitution. Thus in contrast to the enhanced room temperature ferromagnetism in $\text{Bi}(\text{Fe}_{0.95}\text{Co}_{0.05})\text{O}_3$ [21], very weak ferromagnetism was observed in Mn-doped BiFeO_3 , and no cluster spin glass due to canted arranged Fe spins was observed. T_f at around 30 K for $\text{Bi}(\text{Fe}_{0.9}\text{Mn}_{0.1})\text{O}_3$ can be attributed to the ferrimagnetic arranged spins between Mn and Fe ions.

IV. CONCLUSION

$\text{Bi}(\text{Fe}_{1-x}\text{Mn}_x)\text{O}_3$ ceramics (x up to 0.3) were prepared by rapid sintering. Weak ferromagnetism with two magnetic anomalies at low temperatures was observed for $\text{Bi}(\text{Fe}_{0.95}\text{Mn}_{0.05})\text{O}_3$ and $\text{Bi}(\text{Fe}_{0.9}\text{Mn}_{0.1})\text{O}_3$. The stronger paramagnetism is observed for $\text{Bi}(\text{Fe}_{0.7}\text{Mn}_{0.3})\text{O}_3$ indicating a magnetic phase change from antiferromagnetic to paramagnetic with the structure changing from R3c to C222. From temperature-dependent magnetic relaxation measurements, the anomalies at 30 and 140 K are related to the freezing of cluster spin glass.

V. ACKNOWLEDGMENTS

The work was supported by the National Natural Science Foundation of China (No.50802041 and No.50872050), the National Basic Research Program of China (No.2011CB831524), the 2009 Self-Raised Funds Project of Langfang Science and Technology Bureau (No.2009013056), and the 2011 Key Project of the Langfang Teachers College (No.LSZZ201101).

- [1] K. F. Wang, J. M. Liu, and Z. F. Ren, *Adv. Phys.* **58**, 321 (2009).
- [2] D. I. Khomskii, *J. Magn. Magn. Mater.* **306**, 1 (2006).
- [3] G. A. Smolenskii and I. Chupis, *Sov. Phys. Usp.* **25**, 475 (1982).
- [4] J. Wang, J. B. Neaton, H. Zheng, V. Nagarajan, S. B. Ogale, B. Liu, D. Viehland, V. Vaithyanathan, D. G. Schlom, U. V. Waghmare, N. A. Spaldin, K. M. Rabe, M. Wuttig, and R. Ramesh, *Science* **299**, 1719 (2003).
- [5] D. Lebeugle, D. Colson, A. Forget, M. Viret, P. Bonville, J. F. Marucco, and S. Fusil, *Phys. Rev. B* **76**, 024116 (2007).
- [6] T. Kawae, Y. Terauchi, H. Tsuda, M. Kumeda, and A. Morimoto, *Appl. Phys. Lett.* **94**, 112904 (2009).
- [7] D. Lebeugle, D. Colson, A. Forget, M. Viret, A. M. Bataille, and A. Gukasov, *Phys. Rev. Lett.* **100**, 227602 (2008).
- [8] H. Béa, M. Bibes, S. Petit, J. Kreisel, and A. Barthélémy, *Philos. Mag. Lett.* **87**, 165 (2007).
- [9] J. Allibe, I. C. Infante, S. Fusil, K. Bouzehouane, E. Jacquet, C. Deranlot, M. Bibes, and A. Barthélémy, *Appl. Phys. Lett.* **95**, 182503 (2009).
- [10] V. B. Naik and R. Mahendiran, *Solid State Commun.* **149**, 754 (2009).
- [11] V. A. Khomchenko, D. A. Kiselev, M. Kopcewicz, M. Maglione, V. V. Shvartsman, P. Borisov, W. Kleemann, A. M. L. Lopes, Y. G. Pogorelov, J. P. Araujo, R. M. Rubinger, N. A. Sobolev, J. M. Vieira, and A. L. Kholkin, *J. Magn. Magn. Mater.* **321**, 1692 (2009).
- [12] G. L. Yuan, S. W. Or, and H. L. W. Chan, *J. Phys. D* **40**, 1196 (2007).
- [13] J. Huang, Y. Wang, Y. Lin, M. Li, and C. W. Nan, *J. Appl. Phys.* **106**, 063911 (2009).
- [14] G. Catalan and J. F. Scott, *Adv. Mater.* **21**, 2463 (2009).
- [15] D. Lebeugle, D. Colson, A. Forget, M. Viret, P. Bonville, J. F. Marucco, and S. Fusil, *Phys. Rev. B* **76**, 024116 (2007).
- [16] Q. Xu, H. Zai, D. Wu, Y. K. Tang, and M. X. Xu, *J. Alloys Compd.* **485**, 13 (2009).
- [17] Z. X. Cheng, A. H. Li, X. L. Wang, S. X. Doou, K. Ozawa, H. Kimura, S. J. Zhang, and T. R. ShROUT, *J. Appl. Phys.* **103**, 07E507 (2008).
- [18] Y. Wang and C. Nan, *J. Appl. Phys.* **103**, 114104 (2008).
- [19] P. Hermet, M. Goffinet, J. Kreisel, and P. Ghosez, *Phys. Rev. B* **75**, 220102 (2007).
- [20] Y. Yang, J. Y. Sun, K. Zhu, Y. L. Liu, and L. Wan, *J. Appl. Phys.* **103**, 093532 (2008).
- [21] Q. Xu, H. Zai, D. Wu, T. Qiu, and M. X. Xu, *Appl. Phys. Lett.* **95**, 112510 (2009).
- [22] D. Rout, K. Moon, and S. L. Kang, *J. Raman Spectrosc.* **40**, 618 (2009).
- [23] I. Apostolova, A. T. Apostolov, and J. M. Wesselinowa, *J. Phys.: Condens. Matter* **21**, 036002 (2009).
- [24] Y. Sun, M. B. Salamon, K. Garnier, and R. S. Averback, *Phys. Rev. Lett.* **91**, 167206 (2003).
- [25] R. S. Freitas, L. Ghivelder, F. Damay, F. Dias, and L. F. Cohen, *Phys. Rev. B* **64**, 144404 (2001).
- [26] A. Maignan, A. Sundaresan, U. V. Varadaraju, and B. Raveau, *J. Magn. Magn. Mater.* **184**, 83 (1998).
- [27] C. Jaeger, C. Bihler, T. Vallaitis, S. T. B. Goennenwein, M. Open, R. Gross, and M. S. Brandt, *Phys. Rev. B* **74**, 045330 (2006).
- [28] B. Song, J. Jian, H. Bao, M. Lei, H. Li, G. Wang, Y. Xu, and X. Chen, *Appl. Phys. Lett.* **92**, 192511 (2008).
- [29] B. Ramachandran and M. S. R. Rao, *Appl. Phys. Lett.* **95**, 142505 (2009).